Dense-Gas Solvent-Solute Clusters at Near-Infinite Dilution: EPR Spectroscopic Evidence

Claude Carlier and Theodore W. Randolph
Dept. of Chemical Engineering, Yale University, New Haven, CT 06520

The nitrogen hyperfine splitting constant of ditertbutyl nitroxide radicals was measured with electron paramagnetic resonance spectroscopy at near-infinite dilution in near-critical and supercritical ethane, as well as in liquid propane, liquid isobutane, and several nonhydrogen bonding liquid solvents. While the measurements in the liquids are described well by the theory of McRae, large deviations from the liquid behavior are observed in supercritical ethane. The deviations are used as a measure of the effective local density of the solvent around the solute. At the two temperatures investigated, $T_r = 1.009$ and $T_r = 1.084$, the local density enhancement, defined as the ratio of local to bulk densities, exhibits a maximum of about 3 occurring around 1/2 the critical density. The maximum is removed well from the critical density, where the maximum of the isothermal compressibility is observed. Local density enhancements are short-range effects and do not correlate well with the development of long-range critical phenomena. Local density enhancement data in ethane are compared with the prewetting transition that has been observed in near-critical ultrapure argon.

Introduction

In the supercritical fluid state, the solvent properties (such as density, viscosity, and dielectric) are highly sensitive to small changes in pressure or temperature, especially in the immediate vicinity of the critical point. These "tunable" properties make supercritical fluid (SCF) solvents attractive for both separation (McHugh and Krukonis, 1986) and reaction processes (Wu et al., 1991). Commercially successful processes have been developed for SCF extraction. Applications of SCF solvents in reaction processes, however, are only beginning to emerge, and there are not many data available on reactions. Design and control of systems for reactions under supercritical conditions will require not only the same pure-component and mixture thermophysical properties needed for extractions (such as equations of state and mixing rules), but also additional mechanistic information on SCF solvent effects on reactions.

Several studies of reactions revealed large solvent effects on the rate constants which have been explained in terms of "cage effects" or "clustering" of the solvent about solute molecules (Kim and Johnston, 1986; Johnston and Haynes, 1987; Wu et al., 1991; Combes et al., 1992). Solvatochromic (Yonker and Smith, 1988; Kim and Johnston, 1987; Johnston et al., 1989) and fluorescence spectroscopy (Brennecke and Eckert, 1989; Brennecke et al., 1990a; Betts et al., 1992) experiments among others have shown solute-solvent interactions higher than those in homogeneous liquids, leading to the conclusion that effective local solvent or cosolvent densities can be several times higher than the bulk densities. Reaction rates are affected simultaneously through both the rate constants and the local concentrations of the reactants. Because these effects may exhibit opposite pressure dependencies, understanding of the phenomena involved at the molecular level can greatly improve the choice of physical conditions and prediction of reaction rates, and allow the tailoring of SCF solutions for specific applications. Despite the experimental and computational evidence for their existence, solvent-solute clusters have been the subject of a recent debate (Economou and Donohue, 1990; Brennecke et al., 1990b). In examining whether or not solvent-solute clustering is of importance in reactive SCF systems, the distinction must be made between short-range and long-range, or critical and noncritical phenomena. SCF anomalies such as large negative partial molar volumes and large isothermal com-

Correspondence concerning this article should be addressed to T. W. Randolph.

pressibilities result from long-range effects, while local density measurements by various spectroscopic techniques reflect short-range order. The two types of effects may not necessarily be coincident; we will show data from two systems which suggest the contrary.

Background

Several authors reported solvatochromic shifts and fluorescence intensity ratios in supercritical fluids showing deviations from liquid behavior. Early reports gave a qualitative interpretation in terms of a local density higher than the bulk density, but more recently quantitative measurements and more thorough studies have been published.

Using fluorescence spectroscopy, Kajimoto et al. (1988) investigated the charge transfer emission of (*N,N*-dimethylamino)benzonitrile (DMABN) in supercritical CF_3H at $T_r = 1.082$. According to Onsager reaction field theory, the bathochromic shift of the charge-transfer emission is expected to vary linearly with the solvent polarity parameter:

$$\left(\frac{\epsilon - 1}{\epsilon + 2} - \frac{n^2 - 1}{n^2 + 2}\right),$$

where ϵ is the dielectric and n the refractive index of the solvent. While the relationship is reasonably well satisfied for DMABN in several liquid solvents, measurements in supercritical CF_3H reveal a large positive deviation from this line. Starting from a fairly good agreement with the liquid solvent line at high density, the deviation increases as the density is lowered. Eventually, at densities well below the critical density, deviations from the Onsager line begin to decrease. The deviation was attributed to solvent aggregation around the solute, though no estimates of local densities were given.

Smith et al. (1987) and Yonker and Smith (1988) measured solvatochromic shifts for 2-nitroanisole in CO_2, ethane, SF_6 and Xe at reduced temperatures from 1.013 to 1.062. Using the McRae-Bayliss theory (Bayliss and McRae, 1954; McRae, 1956), the authors plotted the Kamlet-Taft parameter π^* as a function of the reaction field and identified two linear regions with different slopes for which no theoretical explanation was given. The break point between the two linear regions in CO_2 at $T_r = 1.013$ occurs at reduced density ρ_r of about 0.6, well-removed from the reduced density near 1, where a maximum in isothermal compressibility and a minimum in solute partial molar volume are seen (Eckert et al., 1986).

Johnston et al. (1989) reevaluated the results of Yonker and Smith, comparing the data to an extrapolation of a line drawn through the data points at the highest densities. Using the deviation from this theoretical line, they explained that the local density ρ^{local} could be estimated as the density of a homogeneous fluid corresponding to a point on the line which gives the same π^* value as the SCF solvent at the bulk density ρ^{bulk}, but they did not report any value. With the same approach, they reviewed the data of Kajimoto et al. and reported a maximum local density enhancement ρ^{local}/ρ^{bulk} of 2.5. This maximum seems to occur at about 1/3 of the critical density, in contrast to Johnston's observation that "in the critical region, clustering increases and decreases rapidly as a function of the solvent compressibility."

Kim and Johnston (1987) also reported their own solvatochromic shift measurements for phenol blue in supercritical ethylene at $T_r = 1.003$ and $T_r = 1.056$. Dimroth-Reichardt E_T values were plotted vs. density, and the curve was compared to the prediction from McRae-Bayliss theory for a homogeneous polarizable dielectric. Agreement with the theoretical curve was very good at high density, but E_T values showed a deviation which got larger as the density was decreased. In their data at $T_r = 1.056$, the local density enhancement ρ^{local}/ρ^{bulk} reached about 1.5 at a reduced bulk density of 0.85, but no maximum was evident in the range investigated ($\rho_r = 0.85$ to 2.1).

For phenol blue in supercritical 1,1-difluoroethane at $T_r = 1.094$ (Johnston and Haynes, 1987), Johnston's results are very similar: the enhancement reached 2.4 for a reduced bulk density of about 0.32, but again no maximum was evident.

Brennecke and Eckert (1989) measured fluorescence intensity ratios I_1/I_4 for naphthalene in CO_2 at $T_r = 1.013$ and 1.046 at a mole fraction of 3.5×10^{-5}. The ratio I_1/I_4 was interpreted as being proportional to local polarity. At constant density, data at $T_r = 1.013$ showed higher local polarities than at $T_r = 1.046$. This deviation was explained in terms of solvent clustering around the solute, but no local density values were reported.

In similar experiments for pyrene in CF_3H at $T_r = 1.013$ and 1.08, CO_2 at $T_r = 1.013$ and 1.063 and ethylene at $T_r = 1.006$ and 1.091, Brennecke et al. (1990a) fitted lines through the higher temperature data in each pair and used these lines as a basis for computing the difference between local and bulk densities. The reported local density augmentations, defined as $(\rho^{local} - \rho^{bulk})$, were compared with the isothermal compressibility and showed a reasonable correspondence, though the maximum in augmentation in ethylene occurred at a lower density than the maximum in isothermal compressibility.

Betts et al. (1992) studied spectral shifts of PRODAN in CF_3H at $T_r = 1.013$ using steady-state fluorescence spectroscopy. Spectral shifts measurements showed that local density deviates from the bulk density and increases as the pressure decreases toward the critical pressure. However, the local density does not return to the bulk density value, if the pressure is further decreased below the critical pressure. Density enhancements ρ^{local}/ρ^{bulk} of up to 2.1 may be calculated from their data, but no maximum is evident.

Knutson et al. (1992) used fluorescence spectroscopy for pyrene in CO_2 at $T_r = 1.02$ and $T_r = 1.14$ and a mole fraction of 3.2×10^{-8}. Assuming that clustering would be minimal at higher temperature, they used deviations from a line through the high-temperature data to compute density enhancements ρ^{local}/ρ^{bulk} as a function of density at $T_r = 1.02$. The resulting curve ρ^{local}/ρ^{bulk} vs. ρ^{bulk} does not show a maximum: the enhancement increases to about 2 at the lowest density investigated ($\rho_r = 0.46$). Molecular dynamics simulations showed a maximum enhancement of about 2.0, occurring around $\rho_r = 0.33$, which, although not explicitly stated, is well-removed from the density at which the maximum in the solvent's isothermal compressibility occurs. The simulations also showed significant enhancements (about 1.5) even at $T_r = 1.14$.

Other computations also have proved to be useful in probing the solvent microstructure around a solute. For example, integral equation approaches (Cochran et al., 1988; Cochran and Lee, 1990) have shown that large excess numbers of solvent can be found surrounding a solute. Debenedetti (1987) has employed fluctuation theory to calculate excesses of over 100

CO_2 solvent molecules around naphthalene, based on partial molar volume data. Similar excesses were calculated from integral equations using Percus-Yevick closure for dilute Ne in Xe, while negative excesses were calculated for the mixture of dilute Xe in Ne (Wu et al., 1990). Molecular dynamics calculations for dilute Ne in supercritical Xe or dilute Xe in supercritical Ne also showed that solvent density around a solute was enhanced or depleted, respectively (Petsche and Debenedetti, 1989).

Finally, using a model for a charged hard-sphere in a compressible dielectric fluid, Wood et al. (1981) calculated a local density of water in the immediate vicinity of an ion of 0.9 g/mL compared to a bulk density of 0.64 g/mL (local density enhancement of 1.4) in the subcritical region at $P_r = 0.79$.

Basis for This Work

To avoid some of the difficulties generally associated with experimental studies of reactions (analysis of the concentrations of the reactants and products, uncertainty about the properties of the transition state, side reactions, and so on), we have chosen to study a simple system: the Heisenberg spin exchange reaction between stable free radicals, that is, ditertbutyl nitroxides (DTBN). This reaction allows us to simultaneously study the effects of pressure and temperature on rate constants and probe the structure around the solute through the effects of solvent polarity in the cybotactic region. Advantages of the system include the fact that concentrations are time-invariant since products are chemically identical to reactants, and the reaction can be studied in a noninvasive fashion using electron paramagnetic resonance (EPR) spectroscopy, a sensitive technique allowing measurements at mole fraction as low as 10^{-7}. We have previously published reaction rate constant data for the spin exchange reaction in supercritical ethane (Randolph and Carlier, 1992). In this work, we examine more closely the local solvent polarity in supercritical ethane.

Frequently employed solvent polarity parameters include the Winstein-Grunwald Y value (Fainberg and Winstein, 1956), the Kosower Z value (Kosower, 1958, 1968) and the Dimroth-Reichardt E_T value (Dimroth et al., 1963), which all probe the cybotactic region around the solute. They are model parameters in the sense that they measure the effect of the solvent polarity on a "model" chemical process. The nitrogen hyperfine splitting constant $\mathfrak{a}_N$ is another probe of local solvent polarity but a nonmodel one. Local polarity affects $\mathfrak{a}_N$ by changing the spin density on nitrogen: higher polarities give increased nitrogen spin densities and higher $\mathfrak{a}_N$ values. $\mathfrak{a}_N$ can be accurately measured by EPR spectroscopy, and Knauer and Napier (1976) showed that it correlates linearly with the E_T values. In liquid solvents, the shift in $\mathfrak{a}_N$ values can therefore be predicted on the basis of this linear relationship and the theory of McRae as follows:

$$\mathfrak{a}_N = a + b\left(\frac{n^2-1}{2n^2+1}\right) + c\left(\frac{\epsilon-1}{\epsilon+2} - \frac{n^2-1}{n^2+2}\right) \tag{1}$$

where n is the refractive index, ϵ is the dielectric, and a, b and c are constants that depend on the nitroxide under investigation. These constants can be determined by a least-squares fit using experimental measurements of $\mathfrak{a}_N$ in different solvents. We measured $\mathfrak{a}_N$ values in several liquid solvents and also used data gathered by Knauer and Napier along with the corresponding dielectric and refractive index data. For molecules with no dipolar moment like ethane or propane, Maxwell's relation ($\epsilon = n^2$) applies and the last term in Eq. 1 becomes zero, yielding:

$$\mathfrak{a}_N = a + b\left(\frac{\epsilon-1}{2\epsilon+1}\right) \tag{2}$$

The dielectric constant can be calculated from the Clausius-Mossotti relation:

$$C_m = \frac{\epsilon-1}{\rho(\epsilon+2)} \tag{3}$$

with C_m given by:

$$C_m = A + B\rho + C\rho^2 + D\ln\left(1+\frac{T_c}{T}\right) + EP \tag{4}$$

Densities are calculated with a modified Benedict-Webb-Rubin equation of state (MBWR) from Younglove and Ely (1987), who also compiled dielectric constant information into the form given by Eqs. 3 and 4 using sources by Weber (1976) for ethane and Goodwin and Haynes (1982a,b) for propane and isobutane. Densities are reported to be accurate to within 5% near the critical point and to within 1.5% (or less depending on the solvent) away from the critical point, while dielectric constants are accurate to within 0.05% and 0.3%, respectively.

At 308 K, the dielectric constant of ethane changes from 1.08 to 1.5 as the pressure increases from 4 to 16 MPa. While this is a small change, the effect on $\mathfrak{a}_N$ values can be detected easily, and information about the local structure will be obtained if deviations from the liquid behavior are observed.

Materials and Methods

X-band EPR spectra were recorded in a Bruker ESP300 EPR spectrometer. Temperatures in the EPR cell were measured with a thermocouple, and the cell was thermostated to ± 0.1 K using a liquid nitrogen boil-off and a Eurotherm temperature controller.

Spectra were measured for solutions at low or very low concentration of DTBN in supercritical ethane, in liquid propane and liquid isobutane away from the critical region, and in diverse solvents which are liquid at room temperature and atmospheric pressure: *n*-pentane, cyclohexane, *n*-heptane, carbon tetrachloride and dimethyl sulfoxide, which will later be referred to as the "liquid solvents."

The experimental apparatus and EPR measurement conditions for the supercritical ethane experiments were described earlier (Randolph and Carlier, 1992). Experiments were conducted in fiberglass tubes at two different temperatures: 308 and 331 K ($T_r = 1.009$ and 1.084, respectively), at pressures varying from 4 MPa to 16 MPa and at nitroxide concentrations ranging from 2×10^{-5} to 9×10^{-4} M. Concentrations were always low enough to be in the one-phase region at all times.

Experiments in isobutane and propane

For these experiments, the fiberglass tube was replaced by

a thick-walled quartz tube (volume, about 0.25 mL) open at one end only. Since equations for density, dielectric constant and viscosity are available, measurements were carried out over a range of temperature, from 200 K up to 283 K for propane and up to 263 K for isobutane, which is well below the boiling point at tank pressure.

At the beginning of each experiment, about 20 μL of a solution of DTBN in *n*-pentane at 10^{-5} M were injected in the tube, and the pentane allowed to evaporate. After the pentane had evaporated, the tube was connected to the high-pressure system. The whole system was first connected to vacuum to remove oxygen and then pressurized with the solvent up to the cylinder pressure. To ensure complete removal of oxygen, the system was once more connected to vacuum and finally repressurized; furthermore, as in the experiments in ethane, the solvent was passed through a scrubber to remove traces of oxygen. Before any spectrum was recorded, the temperature was cycled in the aforementioned range to facilitate mixing. Mole fractions of DTBN did not exceed 10^{-7}.

Experiments in the "liquid solvents"

Measurements were done at one temperature only, either 293.1 or 298.1 K, depending on the availability of data for dielectric constants and using the following procedure: about 20 μL of the solution of DTBN in *n*-pentane at 10^{-5} M were injected in a standard EPR quartz tube (volume, about 2 mL). The pentane was evaporated, and 1 mL of solvent was added. Oxygen was removed by bubbling argon through the solution for about 3 minutes. The EPR spectrum was recorded after allowing the temperature in the EPR cell to stabilize.

All EPR spectra were recorded using a modulation amplitude of 0.5 Gauss, a modulation frequency of 100 kHz, a time constant of 0.01 ms, and microwave power of 10 mW. The center field was set at 3440 Gauss. Most spectra were 60 Gauss wide, recorded in 20-second single scans except in a few cases, where the signal had to be accumulated due to the very low concentration of DTBN. Digitized spectra were transferred to a Hewlett Packard 720 workstation. Simulated EPR spectra were fit to experimental spectra using modified programs based on the EPR simulation programs of Schneider and Freed (1989). For ethane, the spin exchange rate per molecule and the nitrogen hyperfine splitting constant $\mathfrak{A}_N$ were varied. Linewidth corrections for spin-rotation interactions (Atkins and Kivelson, 1966; Plachy and Kivelson, 1967) as a function of T/η were made by measuring the linewidth in the absence of spin exchange at a maximum mole fraction of 10^{-6}. For propane, isobutane and the liquid solvents, the parameters used for the fit were the intrinsic linewidth and the hyperfine splitting constant, since at the concentration used DTBN is nearly at infinite dilution and there is no measurable spin exchange.

Results and Discussion

Experimental $\mathfrak{A}_N$ values in liquid propane, isobutane, *n*-pentane, cyclohexane, *n*-heptane, carbon tetrachloride, and dimethyl sulfoxide, as well as values reported by Knauer and Napier for 16 nonhydrogen bonding solvents are given in Tables 1 and 2. For propane and isobutane, the dielectric constant ϵ was calculated as a function of T and P with the MBWR equation of state, and Eqs. 3 and 4. The refractive index n was calculated as the square root of the dielectric according to Maxwell's equation. Although it is not rigorous for isobutane, the dipole moment of isobutane (0.1 D) is low enough for this relation to give a very reasonable estimation of n. For the other solvents, the dielectric constant data were found in the Landolt-Börnstein tables (1991). The refractive indices for the D line of sodium were found in the *International Critical Tables of Numerical Data, Physics, Chemistry and Technology* (West and Hull, 1933). [For reference on Clausius-Mossotti and Maxwell's relations, consult *Theory of Electric Polarization* (Böttcher, 1973) and *Techniques of Chemistry* (Weissberger and Rossiter, 1972).] These values were used to determine the constants a, b and c in Eq. 1. The constants determined by nonlinear least-squares fit are: $a=14.7$, $b=2.56$, and $c=0.66$, with a correlation coefficient $r=0.97$. Figure 1 shows the experimental vs. calculated $\mathfrak{A}_N$ for these values of the coefficients.

Table 1. Nitrogen Hyperfine Splitting Constant $\mathfrak{A}_N$ of DTBN in Various Solvents (Data from Knauer and Napier, 1976)

No.	Solvent	Dielectric Constant, ϵ	Refractive Index, n_D	$\mathfrak{A}_N$ (G)
1	*n*-hexane	1.8891	1.37536	15.134
2	carbon tetrachloride	2.24	1.4656	15.331
3	carbon disulfide	2.6387	1.6295	15.289
4	toluene	2.392	1.49782	15.347
5	benzene	2.2824	1.50144	15.404
6	diethyl ether	4.38	1.35424	15.334
7	chlorobenzene	5.6899	1.52479	15.472
8	bromobenzene	5.42	1.55977	15.479
9	pyridine	13.28	1.50919	15.608
10	acetophenone	18.2	1.53427	15.562
11	1,2-dichloroethane	10.55	1.44432	15.655
12	acetone	21.29	1.35886	15.527
13	*N,N*-dimethyl formamide	37.11	1.42938	15.635
14	acetonitrile	37.65	1.34596	15.666
15	nitromethane	37.34	1.38133	15.759
16	DMSO	47.54	1.4770	15.692

Since ethane has no dipolar moment, the hyperfine splitting constants $\mathfrak{A}_N$ measured in SCF ethane are plotted directly vs. $(\epsilon-1)/(2\epsilon+1)$ and compared to the line for liquid solvents, as given by Eq. 2. Large deviations from this line can be seen in Figure 2 at the two different experimental temperatures, 308 and 331 K. At high density, the $\mathfrak{A}_N$ values are close to the values expected in a liquid but get much larger as the density is decreased toward the critical pressure. At still lower densities, $\mathfrak{A}_N$ values again approach the line.

In ethane, the quotient $(\epsilon-1)/(2\epsilon+1)$ is very nearly proportional to density. Thus, $\mathfrak{A}_N$ values deviations provide a measure of the local solvent density "felt" by the nitroxide. As shown in Figure 3, it is more instructive to plot the experimental points $\mathfrak{A}_N$ directly vs. the reduced density of ethane and to transform the line for liquid solvents into the curve $\mathfrak{A}_N=f(\rho_r)$ using Eqs. 2, 3 and 4. The deviation of the $\mathfrak{A}_N$ values from linearity near the critical point indicates that the effective local ethane density measured by $\mathfrak{A}_N$ is higher than the bulk density predicted by the equation of state. This is similar to the nonlinearities in E_T values observed by Johnston and Haynes (1987), Kim and Johnston (1987), and Kajimoto et al. (1988). Each experimental point consists of an $\mathfrak{A}_N$ value, which is a measure of the direct environment of the nitroxide molecule, associated with the bulk density of the solvent computed from the measured T and P. The effective local density

Table 2. Nitrogen Hyperfine Splitting Constant a_N of DTBN in Liquid Propane, Liquid Isobutane and Liquid Solvents

Solvent	T (K)	P (MPa)	Density (mol/L)	Dielectric Constant, ϵ	Refractive Index n_D	a_N (G)
propane	203.0	0.67	13.90	1.85807	1.3631	15.1832
	213.0	0.67	13.66	1.83901	1.3561	15.1661
	223.0	0.67	13.40	1.81974	1.3490	15.1549
	233.0	0.67	13.14	1.80018	1.3417	15.1479
	243.0	0.67	12.88	1.78023	1.3343	15.1391
	253.0	0.69	12.60	1.75981	1.3266	15.1314
	263.0	0.70	12.31	1.73870	1.3186	15.1231
	273.0	0.72	12.01	1.71677	1.3103	15.1190
	283.0	0.73	11.69	1.69370	1.3014	15.1155
isobutane	253.0	0.21	10.38	1.83620	1.3551	15.1315
	243.0	0.21	10.56	1.85521	1.3621	15.1391
	233.0	0.21	10.74	1.87404	1.3690	15.1481
	223.0	0.21	10.92	1.89275	1.3758	15.1659
	213.0	0.21	11.09	1.91141	1.3825	15.1816
	203.0	0.21	11.27	1.93008	1.3893	15.2005
	218.0	0.20	11.01	1.90207	1.3792	15.1760
	228.0	0.20	10.83	1.88339	1.3724	15.1615
	238.0	0.20	10.65	1.86463	1.3655	15.1584
	248.0	0.20	10.47	1.84571	1.3586	15.1536
	253.0	0.20	10.38	1.83618	1.3551	15.1371
	263.0	0.20	10.19	1.81689	1.3479	15.1337
	258.0	0.16	10.28	1.82649	1.3515	15.1312
n-pentane (17)	293.1	0.1	8.679	1.8471	1.3570	15.1473 ± 5.10^{-4}
cyclohexane (18)	293.1	0.1	9.250	2.03835	1.43119	15.1709
n-heptane (19)	293.1	0.1	6.823	1.9180	1.3867	15.2188 ± 2.10^{-4}
CCl_4 (2)	293.1	0.1	10.36	2.24	1.4656	15.3458 ± 3.10^{-4}
DMSO (16)	293.1	0.1	14.03	47.54	1.4770	15.6893

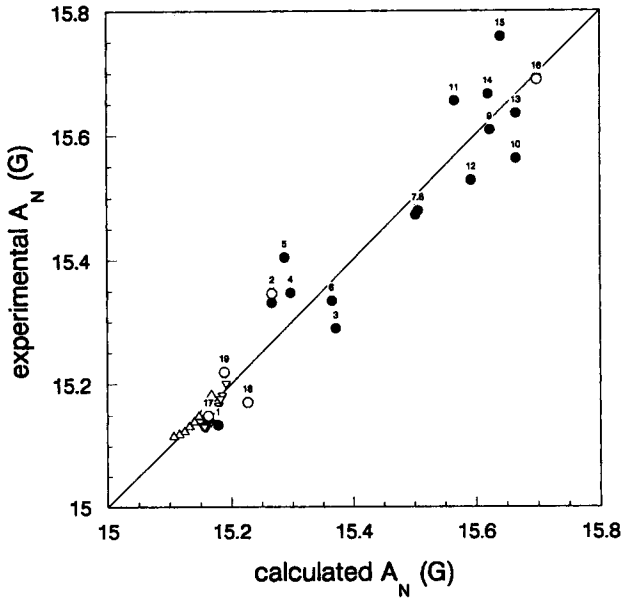

Figure 1. Experimental nitrogen hyperfine splitting constant a_N vs. a_N calculated with Eq. 1 and the least-squares fit coefficients *a*, *b* and *c* for DTBN in liquids.

Data from Knauer and Napier (1976, ●), propane (▵), isobutane (▿), and liquid solvents (○). See Tables 1 and 2 for the correspondence between indices and solvents. Lines joining the data points are only a guide to the eye.

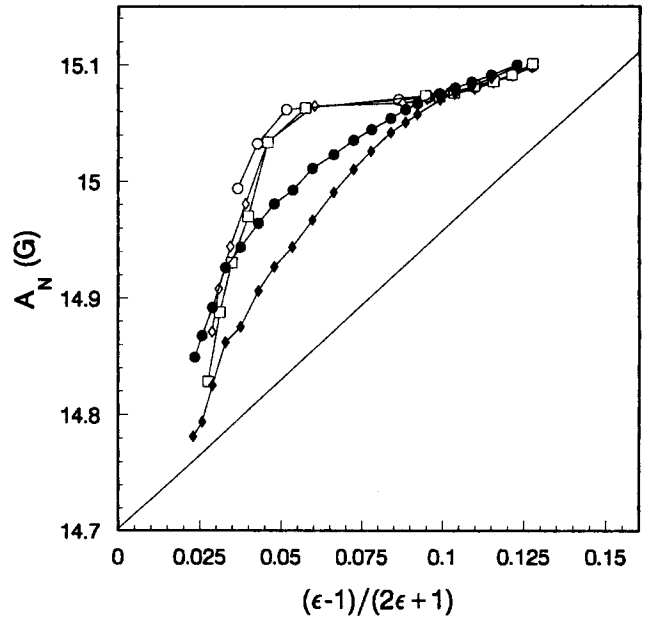

Figure 2. Nitrogen hyperfine splitting constant a_N vs. $(\epsilon-1)/(2\epsilon+1)$ for DTBN in ethane and line given by Eq. 2 for homogeneous liquids with no dipolar moment.

At 308 K, concentrations are 2.6×10^{-4} M (○), 6×10^{-4} M (◇), 6.6×10^{-4} M (□). At 331 K, concentrations are 3.9×10^{-4} M (●), 8.9×10^{-4} M (◆). Lines joining the data points are only a guide to the eye.

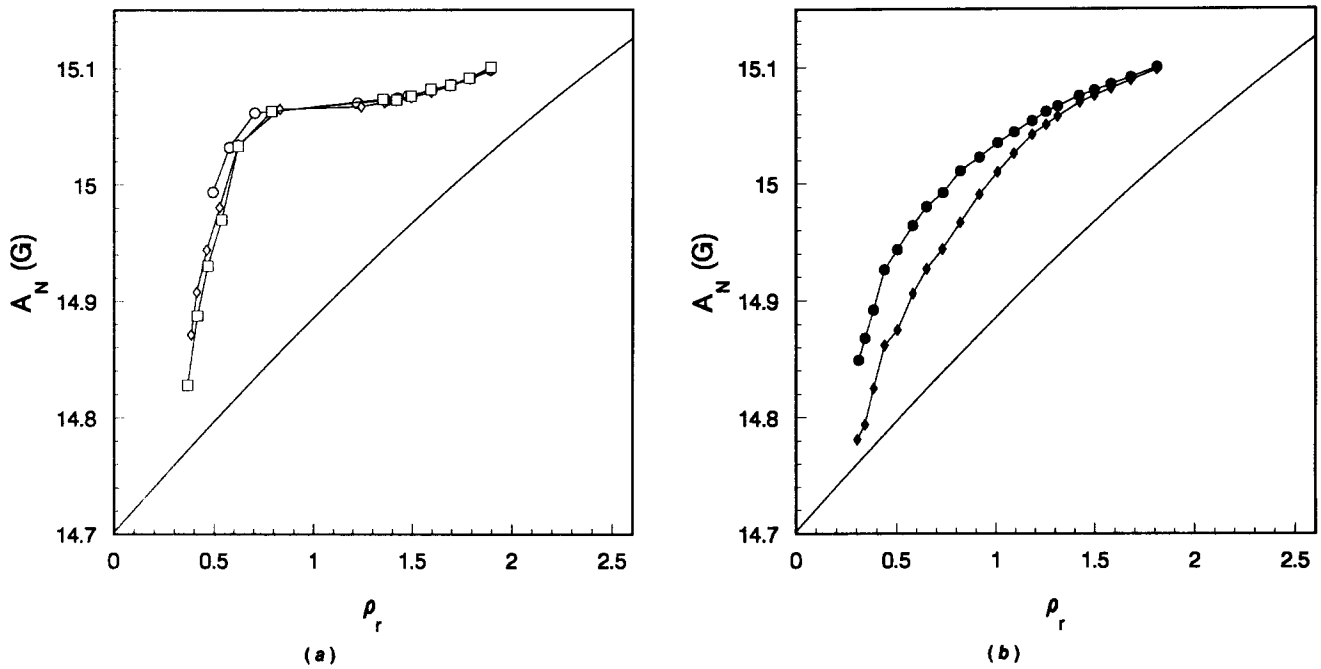

Figure 3. Nitrogen hyperfine splitting constant $\mathcal{A}_N$ vs. reduced density ρ_r for DTBN in ethane and curve $\mathcal{A}_N = f(\rho_r)$: (a) 308 K, (b) 331 K.

Symbols are the same as in Figure 2. Lines joining the data points are only a guide to the eye.

is then obtained as the density of an hypothetical liquid ethane solution which would give the same $\mathcal{A}_N$ value.

After computing the local density for all the experimental points, the "local density enhancement," defined as the ratio of the effective local density ρ^{local} to the bulk density ρ^{bulk} is plotted vs. the reduced bulk density of ethane for the two different temperatures, as shown in Figures 4a and 4b. A maximum enhancement of about 3 occurs between 0.4 and 0.6 times the critical density. Thus, the maximum local density is about 12 mol/L, a value very similar to that for liquid ethane.

It is important to note that the maximum enhancement occurs at a bulk density lower than the critical density, in qualitative agreement with molecular dynamics results on the pyrene-CO_2 system by Knutson et al., which show a maximum

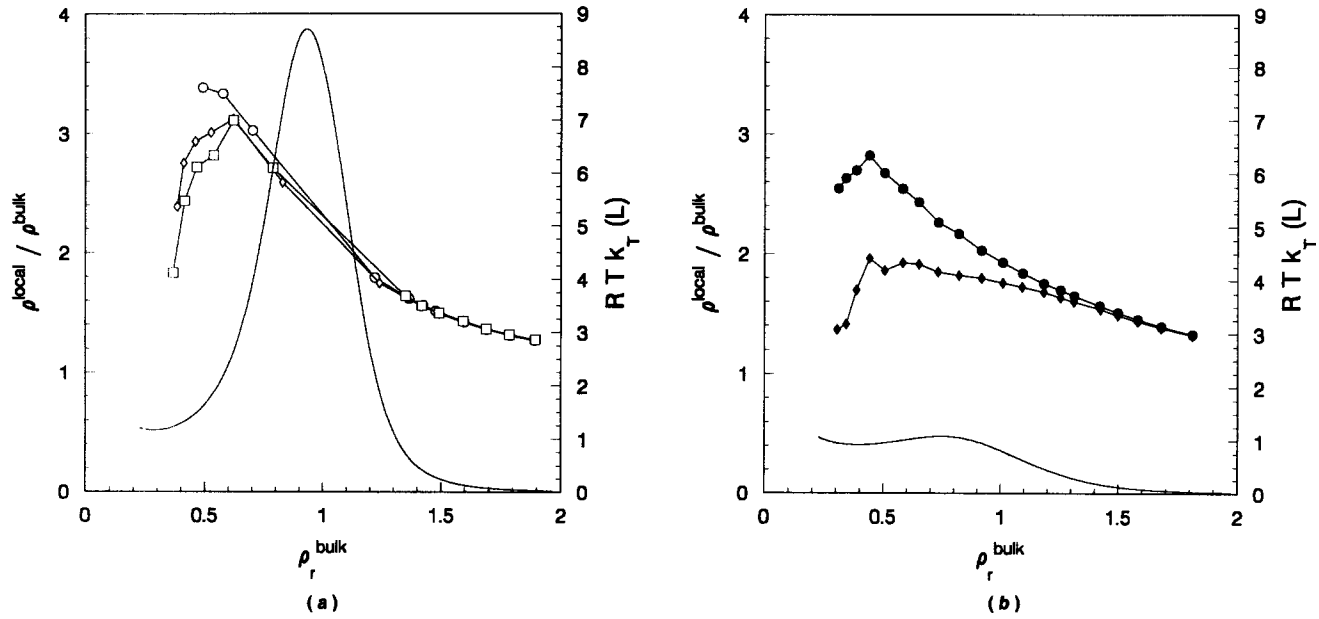

Figure 4. ρ^{local}/ρ^{bulk} vs. reduced bulk density ρ_r^{bulk} for DTBN in ethane and isothermal compressibility k_T vs. ρ_r^{bulk} (solid line): (a) 308 K, (b) 331 K.

Symbols are the same as in Figure 2. Lines joining the data points are only a guide to the eye.

occurring at about 1/3 the critical density. The maximum does not correspond to the maximum for the isothermal compressibility, which for reference is also plotted in Figures 4a and 4b. There appears to be significant enhancement even at 331 K ($T_r = 1.08$). The simulation results also indicated enhancement at $T_r = 1.14$, although Knutson et al. assumed that there would be none to analyze their fluorescence data.

Contrary to the molecular dynamics results of Knutson et al., which predict that ρ^{local}/ρ^{bulk} is greater than unity even at zero bulk density, the experimentally measured value of ρ^{local}/ρ^{bulk} approaches 1 rapidly at lower densities. This is probably not due to a fundamental disagreement between the simulation and the experiments, but rather a question of definition: the local enhancement of Knutson et al. is calculated by assuming an arbitrary (but fixed) size of the cybotactic region about the solute. The contents of this fixed-volume region comprise the local density; in the experiments, the size of the solvent shell that the nitroxide can "feel" is likely to be density-dependent.

Kim and Johnston (1987) defined a degree of clustering $(\rho^{local} - \rho^{bulk})/\rho^{bulk}$ and proposed that it could be related to the isothermal compressibility k_T by:

$$\frac{(\rho^{local} - \rho^{bulk})}{\rho^{bulk}} = \frac{1}{V_{12}} (kTk_T - \overline{V}_2^{\infty}) \tag{5}$$

or assuming a linear relation between $\overline{V}_2^{\infty}$ and k_T, as:

$$\frac{(\rho^{local} - \rho^{bulk})}{\rho^{bulk}} = ak_T + b \tag{6}$$

which predicts that the maximum of the density enhancement should occur at the maximum of the isothermal compressibility. However, our results, in agreement with the simulations of Knutson et al. (1992), show a maximum occurring below the critical density, not at the maximum of k_T. The maximum in ρ^{local}/ρ^{bulk} is due to preferential filling of the cybotactic region of the probe molecule by solvent molecules. This short-range structure results in a finite local density enhancement to near liquid-like densities about the probe molecule and is not directly related to the long-range fluctuations that give rise to the maximum in isothermal compressibility. The local density reported by cybotactic probes must remain finite, while k_T diverges at the critical point.

Analogy to Prewetting Transitions

Economou and Donohue (1990) suggested that local density augmentation need not be invoked to explain the large infinite-dilution partial molar volumes of solutes near the solvent's critical point. In addition, they state that "while there can be enhancement in solvent density in the vicinity of a solute molecule near the solvent critical point, the magnitude is small compared to the mean field effect." However, we find it difficult to explain our results in terms of mean field effects. At $T_r = 1.08$ and a DTBN mole fraction below 10^{-5}, effective local densities of ethane reach nearly three times the bulk value. Because this maximum in local density does not correspond with the minimum in partial molar volume (which scales as the maximum in isothermal compressibility), it is unlikely that the effect can be explained as a mean field effect. Indeed, because the local density effect on $\mathfrak{A}_N$ falls off with an r^{-6} dependence (Wertz and Bolton, 1986), the observed enhancements must be due to a short-range structural change and not a long-range mean field effect.

Ascarelli and Nakanishi (1990) measured the dielectric constant of ultrapure argon (O_2 concentration was estimated to be about 1 ppb) near the critical point along the isobars $P_r = 1.033$ and 1.136. In Figure 5 we have replotted their data in terms of local density enhancement ρ^{local}/ρ^{bulk}, along with the isothermal compressibility k_T, calculated using a 32-parameter MBWR equation of state (Younglove, 1982). The local densities, as measured by the dielectric in the immediate vicinity of the surface of a platinum photocathode, agree very well with the bulk densities calculated from the equation of state at high and low densities but show large deviations in the intermediate region $\rho_r = 0.5$-1.5. The deviation suggests a prewetting transition and was explained in terms of the interaction between the randomly oriented dipole moments of the argon atoms and their image in the metal. It is interesting to note that the maximum of the local density enhancement occurs at a reduced density below 1 and does not correlate with the isothermal compressibility. Indeed, as the critical point is approached, the maximum of the enhancement shifts away from the maximum of k_T. The effect is necessarily short-ranged in nature, and in this ultrapure environment cannot be attributed to large negative partial molar volumes of a solute.

By analogy, we suggest that the high local densities of ethane around DTBN that we observe are the result of a similar prewetting transition wherein a layer of ethane fills (at least) the first solvent shell to liquid-like densities, although the bulk ethane density is less than 1/3 of that of the liquid. Because the effect of local density on $\mathfrak{A}_N$ falls off so sharply with distance we are unable to say how far away from a DTBN molecule such enhancement would persist. However, based on preliminary molecular dynamics and Monte-Carlo simulation results performed in our laboratory for Lennard-Jones mol-

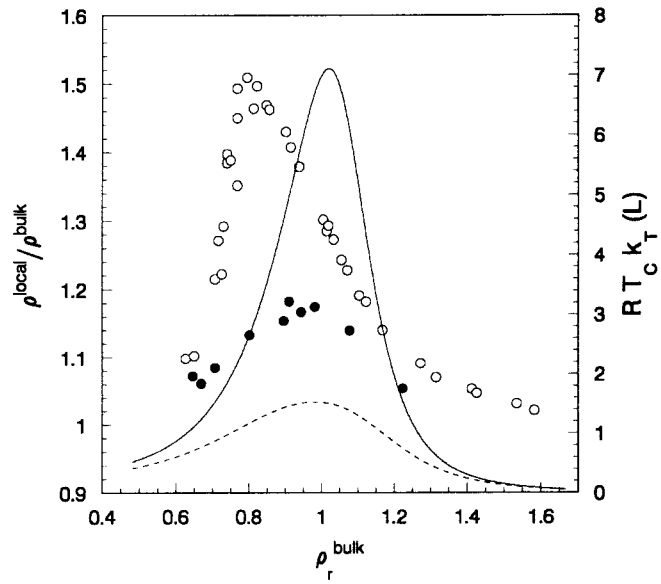

Figure 5. Local density enhancement ρ^{local}/ρ^{bulk} vs. reduced bulk density ρ_r^{bulk} for pure argon.

At $P_r = 1.033$ (○) and $P_r = 1.136$ (●) and isothermal compressibility k_T vs. reduced bulk density ρ_r^{bulk} at $P_r = 1.033$ (——) and $P_r = 1.136$ (----).

ecules with parameters approximating the ethane-DTBN system, we do not expect local density to be greatly perturbed for more than two or three solvent shells.

Conclusions

Large augmentations of local densities of ethane around DTBN molecules are evident in our experiments. The maximum in density does not correlate well with the maximum in isothermal compressibility. Thus, unlike the large partial molar volumes seen in supercritical systems, the local density augmentation is not the result of a long-range critical effect, but rather a short-range structural effect, as suggested by Kajimoto et al. (1988) and Knutson et al. (1992). Such short-range effects involve the preferential filling of the first few solvent shells around a solute and are analogous with prewetting transitions observed on platinum surfaces in ultrapure argon.

Reactions are more likely to be influenced by short-ranged solvent structure than by long-ranged density fluctuations. Experimentally we have observed that the enhanced local densities of solvent around nitroxide free radicals lead to longer collision times and hence enhanced reaction rate constants (Randolph and Carlier, 1992); continuing experiments are under way to further "tune" our solvent for these reactions with the addition of cosolvents. In addition, we are currently using molecular dynamics simulations to probe local density augmentation effects on the dynamics of very fast free-radical reactions under supercritical conditions.

Acknowledgment

Acknowledgment is made to the donors of the Petroleum Research Fund, administered by the American Chemical Society, for partial support of this work. Further acknowledgment is made to the National Science Foundation for their support (Grant BCS-9014119 and a Presidential Young Investigator Award).

Notation

$\mathcal{A}_N$ = nitrogen hyperfine splitting constant
C_m = Clausius-Mossotti function
k = Boltzmann's constant
k_T = isothermal compressibility
n = refractive index
P = pressure
T = temperature
V_{12} = coordination volume with radius r_{12}
$\overline{V}_2^{\infty}$ = partial molar volume of component 2 (solute) at infinite dilution
r = molecular separation distance

Greek letters

ϵ = dielectric constant
η = viscosity
ρ^{bulk} = bulk density
ρ^{local} = local density

Subscripts

c = critical value
r = reduced value

Literature Cited

Ascarelli, G., and H. Nakanishi, "Prewetting Transition in Supercritical Argon," *J. Phys. France*, **51**, 341 (1990).

Atkins, P. W., and D. Kivelson, "ESR Linewidths in Solution: II. Analysis of Spin-Rotational Relaxation Data," *J. Chem. Phys.*, **44**, 169 (1966).

Bayliss, N. S., and E. G. McRae, "Solvent Effects in Organic Spectra: Dipole Forces and the Franck-Condon Principle," *J. Phys. Chem.*, **58**, 1002 (1954).

Betts, T. A., J. Zagrobelny, and F. V. Bright, "Elucidation of Solute-Fluid Interactions in Supercritical CF_3H by Steady-State and Time-Resolved Fluorescence Spectroscopy," *ACS Symp. Proc.*, **488**, 48 (1992).

Böttcher, C. J. F., *Theory of Electric Polarization*, Elsevier, Amsterdam (1973).

Brennecke, J. F., and C. A. Eckert, "Fluorescence Spectroscopy Studies of Intermolecular Interactions in Supercritical Fluids," *Supercritical Fluid Science and Technology*, K. P. Johnston and J. M. L. Penninger, eds., *ACS Symp. Ser.*, **406**, 14 (1989).

Brennecke, J. F., D. L. Tomasko, J. Peshkin, and C. A. Eckert, "Fluorescence Spectroscopy Studies of Dilute Supercritical Solutions," *Ind. Eng. Chem. Res.*, **29**, 1682 (1990a).

Brennecke, J. F., P. G. Debenedetti, C. A. Eckert, and K. P. Johnston, "Letters to the Editor," *AIChE J.*, **36**(12), 1927 (1990b).

Cochran, H. D., L. L. Lee, and D. M. Pfund, "Study of Fluctuations in Supercritical Solutions by an Integral Equation Method," *Proc. Int. Symp. on Supercrit. Fluids*, F. Perrut, ed., Nice, France, p. 245 (1988).

Cochran, H. D., and L. L. Lee, "Structure and Properties of Supercritical Fluid Mixtures from Kirkwood-Buff Fluctuation Theory and Integral Equation Methods," *Fluctuation Theory of Mixtures*, E. Matteoli and G. A. Mansoori, eds.,Taylor and Francis, New York, p. 69 (1990).

Combes, J. R., K. P. Johnston, K. E. O'Shea, and M. A. Fox, "The Influence of Solvent-Solute and Solute-Solute Clustering on Chemical Reactions in Supercritical Fluids," *Supercritical Fluid Technology*, F. V. Bright and M. E. P. McNally, eds., *ACS Symp. Ser.*, **488**, 31 (1992).

Debenedetti, P. G., "Clustering in Dilute, Binary Supercritical Fluid Mixtures: A Fluctuation Analysis," *Chem. Eng. Sci.*, **42**, 2203 (1987).

Dimroth, K., C. Reichardt, T. Siepmann, and F. Bohlmann, *Justus Liebigs Ann. Chem.*, **661**, 1 (1963).

Eckert, C. A., D. H. Ziger, K. P. Johnston, and S. Kim, "Solute Partial Molal Volumes in Supercritical Fluids," *J. Phys. Chem.*, **90**, 2738 (1986).

Economou, I. G., and M. D. Donohue, "Mean Field Calculations of Thermodynamic Properties of Supercritical Fluids," *AIChE J.*, **36**(12), 1920 (1990).

Fainberg, A. H., and S. Winstein, "Correlation of Solvolysis Rates: III. *t*-butyl Chloride in a Wide Range of Solvent Mixtures," *J. Amer. Chem. Soc.*, **78**, 2770 (1956).

Goodwin, R. D., and W. M. Haynes, "Thermophysical Properties of Propane from 85 to 700 K at Pressures to 70 MPa," *Nat. Bur. Std. (U.S.) Monogr.*, 170 (1982a).

Goodwin, R. D., and W. M. Haynes, "Thermophysical Properties of Isobutane from 114 to 700 K at Pressures to 70 MPa," *Nat. Bur. Std. (U.S.) Tech. Note*, 1051 (1982b).

Johnston, K. P., and C. Haynes, "Extreme Solvent Effects on Reaction Rate Constants at Supercritical Fluid Conditions," *AIChE J.*, **33**, 2017 (1987).

Johnston, K. P., S. Kim, and J. Combes, "Spectroscopic Determination of Solvent Strength and Structure in Supercritical Fluid Mixtures: A Review," *Supercritical Fluid Science and Technology*, K. P. Johnston and J. M. L. Penninger, eds., *ACS Symp. Ser.*, **406**, 52 (1989).

Kajimoto, O., M. Futakami, T. Kobayashi, and K. Yamasaki, "Charge-Transfer-State Formation in Supercritical Fluid: (*N*,*N*-Dimethylamino)benzonitrile in CF_3H," *J. Phys. Chem.*, **92**, 1347 (1988).

Kim, S., and K. P. Johnston, "Effects of Supercritical Solvents on the Rates of Homogeneous Chemical Reactions," *ACS Symp. Ser.*, **329** (1986).

Kim, S., and K. P. Johnston, "Molecular Interactions in Dilute Supercritical Fluid Solutions," *Ind. Eng. Chem. Res.*, **26**, 1206 (1987).

Knauer, B. R., and J. J. Napier, "The Nitrogen Hyperfine Splitting Constant of the Nitroxide Functional Group as a Solvent Polarity Parameter: The Relative Importance for a Solvent Polarity Parameter of Its Being a Cybotactic Probe vs. Its Being a Model Process," *J. Amer. Chem. Soc.*, **98**, 4395 (1976).

Knutson, B. L., D. L. Tomasko, C. A. Eckert, P. G. Debenedetti, and A. A. Chialvo, "Local Density Augmentation in Supercritical Solutions: A Comparison between Fluorescence Spectroscopy and Molecular Dynamics Results," *Supercritical Fluid Technology*, F. V. Bright and M. E. P. McNally, eds., *ACS Symp. Ser.*, **488**, 60 (1992).

Kosower, E. M., "The Effect of Solvent on Spectra: I. A New Empirical Measure of Solvent Polarity: Z-Values," *J. Amer. Chem. Soc.*, **80**, 3253 (1958).

Kosower, E. M., *An Introduction to Physical Organic Chemistry*, Wiley, New York (1968).

Landolt-Börnstein, *Numerical Data and Functional Relationships in Science and Technology*, New Series IV/6, O. Madelung, ed., Springer Verlag, New York (1991).

McHugh, M. A., and V. J. Krukonis, *Supercritical Fluid Extraction: Principles and Practice*, Butterworths, Boston (1986).

McRae, E. G., "Theory of Solvent Effects on Molecular Electronic Spectra: Frequency Shifts," *J. Phys. Chem.*, **61**, 562 (1956).

Petsche, I. B., and P. G. Debenedetti, "Solute-Solvent Interactions in Infinitely Dilute Supercritical Mixtures: A Molecular Dynamics Investigation," *J. Chem. Phys.*, **91**, 7075 (1989).

Plachy, W., and D. Kivelson, "Spin Exchange in Solutions of di-Tertiary-Butyl Nitroxide," *J. Chem. Phys.*, **47**, 3312 (1967).

Randolph, T. W., and C. Carlier, "Free-Radical Reactions in Supercritical Ethane: A Probe of Supercritical Fluid Structure," *J. Phys. Chem.*, **96**, 5146 (1992).

Schneider, D. J., and J. H. Freed, "Calculating Slow Motional Magnetic Resonance Spectra," *Biological Magnetic Resonance*, Vol. 8, L. J. Berliner and J. Reubens, eds., Plenum Press, New York (1989).

Smith, R. D., S. L. Frye, C. R. Yonker, and R. W. Gale, "Solvent Properties of Supercritical Xe and SF_6," *J. Phys. Chem.*, **91**, 3059 (1987).

Weber, L. A., "Dielectric Constant Data and the Derived Clausius-Mossotti Function for Compressed Gaseous and Liquid Ethane," *J. Chem. Phys.*, **65**, 446 (1976).

Weissberger, A., and B. W. Rossiter, eds., *Techniques of Chemistry*, Vol. I, Part IV, Chaps. V and VI, Wiley-Interscience, New York (1972).

Wertz, J. E., and J. R. Bolton, *Electron Spin Resonance*, McGraw-Hill, New York (1972).

West, C. J., and C. Hull, eds., *International Critical Tables of Numerical Data, Physics, Chemistry and Technology*, Vol. VI, U.S. National Research Council by McGraw-Hill, New York (1933).

Wood, R. H., J. R. Quint, and J-P. E. Grolier, "Thermodynamics of a Charged Hard Sphere in a Compressible Dielectric Fluid: A Modification of the Born Equation To Include the Compressibility of the Solvent," *J. Phys. Chem.*, **85**, 3944 (1981).

Wu, R.-S., L. L. Lee, and H. D. Cochran, "Structure of Dilute Supercritical Solutions: Clustering of Solvent and Solute Molecules and the Thermodynamic Effects," *Ind. Eng. Chem. Res.*, **29**, 977 (1990).

Wu, B. C., S. C. Paspek, M. T. Klein, and C. LaMarca, "Reactions In and With Supercritical Fluids," *Supercritical Fluid Technology: Reviews in Modern Theory and Applications*, T. J. Bruno and J. F. Ely, eds., CRC Press, Boston (1991).

Wu, B. C., M. T. Klein, and S. T. Sandler, "Solvent Effects on Reactions in Supercritical Fluids," *Ind. Eng. Chem. Res.*, **30**, 822 (1991).

Yonker, C. R., and R. D. Smith,"Solvatochromism: A Dielectric Continuum Model Applied to Supercritical Fluids," *J. Phys. Chem.*, **92**, 235 (1988).

Younglove, B. A., "Thermophysical Properties of Fluids: I. Argon, Ethylene, Parahydrogen, Nitrogen, Nitrogen Trifluoride, and Oxygen," *J. Phys. Chem. Ref. Data*, **11**, Supp. 1 (1982).

Younglove, B. A., and J. F. Ely, "Thermophysical Properties of Fluids: II. Methane, Ethane, Propane, Isobutane, and Normal Butane," *J. Phys. Chem. Ref. Data*, **16**, 577 (1987).

Manuscript received Aug. 3, 1992, and revision received Oct. 19, 1992.